RSC Advances

PAPER

View Article Online
View Journal | View Issue

Cite this: *RSC Adv.*, 2015, **5**, 101370

Assessment of density functional methods for exciton binding energies and related optoelectronic properties†

Jui-Che Lee,[a] Jeng-Da Chai*[b] and Shiang-Tai Lin*[a]

Received 29th September 2015
Accepted 18th November 2015

DOI: 10.1039/c5ra20085g

www.rsc.org/advances

The exciton binding energy, the energy required to dissociate an excited electron–hole pair into free charge carriers, is one of the key factors to the optoelectronic performance of organic materials. However, it remains unclear whether modern quantum-mechanical calculations, mostly based on Kohn–Sham density functional theory (KS-DFT) and time-dependent density functional theory (TDDFT), are reliably accurate for exciton binding energies. In this study, the exciton binding energies and related optoelectronic properties (*e.g.*, the ionization potentials, electron affinities, fundamental gaps, and optical gaps) of 121 small- to medium-sized molecules are calculated using KS-DFT and TDDFT with various density functionals. Our KS-DFT and TDDFT results are compared with those calculated using highly accurate CCSD and EOM-CCSD methods, respectively. The ωB97, ωB97X, and ωB97X-D functionals are shown to generally outperform (with a mean absolute error of 0.36 eV) other functionals for the properties investigated.

I. Introduction

An exciton, a bound electron–hole pair, can be generated when light is absorbed in a photoactive material. The electron–hole pair may be located at the same molecular unit (*e.g.*, a Frenkel exciton) or different molecular units (*e.g.*, an intermolecular charge-transfer exciton).[1] The Coulomb interaction that stabilizes the exciton with respect to free electrons and holes is known as the exciton binding energy.[2] Materials with small exciton binding energies usually exhibit high charge separation efficiency,[3] which are often desirable for photovoltaic applications, whereas the opposite may be favorable for light-emitting devices.[1] Covalently bounded inorganic semiconductors have delocalized charge carriers and broad valence and conduction bands with exciton binding energies being as small as a few millielectron volts (meV). In contrast, the electronic properties of organic semiconductors are dominated by the localized charge on individual molecules and the large polarizabilities.[4,5] As a result, the exciton binding energies of organic semiconductors can be as large as 0.1–1 eV. Therefore, it is important to develop a comprehensive understanding of the relevant parameters controlling the exciton binding energies of organic materials for the design of ideal photoactive material.

While a direct measurement of the exciton binding energy may be challenging, the exciton binding energy can be obtained from the difference between the fundamental and optical gaps, each of which can be measured directly.[4,6–9] On the other hand, the fundamental and optical gaps can also be calculated using quantum-mechanical methods. Nayak *et al.* calculated the exciton binding energies of small organic conjugated molecules in vacuum and in thin films[10,11] using Kohn–Sham density functional theory (KS-DFT)[12,13] and time-dependent density functional theory (TDDFT)[14,15] with the B3LYP functional.[16,17] However, the overall accuracy of KS-DFT and TDDFT with conventional density functionals is not comprehensively examined on exciton binding energies.

While intermolecular charge-transfer excitons are also important, in this work, we only focus on the Frenkel excitons. Specifically, we examine the accuracy of exciton binding energies and related optoelectronic properties on a diverse range of molecules using KS-DFT and TDDFT with several widely used density functionals. The rest of this paper is organized as follows. In Section II, we describe our test sets and computational details. The exciton binding energies and related optoelectronic properties obtained from density functional methods are compared with those obtained from high-level *ab initio* methods in Section III. Our conclusions are given in Section IV.

[a]*Department of Chemical Engineering, National Taiwan University, Taipei 10617, Taiwan. E-mail: stlin@ntu.edu.tw*

[b]*Department of Physics, Center for Theoretical Sciences, Center for Quantum Science and Engineering, National Taiwan University, Taipei 10617, Taiwan. E-mail: jdchai@phys.ntu.edu.tw*

† Electronic supplementary information (ESI) available. See DOI: 10.1039/c5ra20085g

II. Test sets and computational details

To evaluate the performance of the functionals on exciton binding energies and related optoelectronic properties (*e.g.*, vertical ionization potentials, vertical electron affinities, fundamental gaps, optical gaps, and exciton binding energies), we collect a test set, which consists of experimental vertical ionization potentials of 121 small- to medium-sized molecules in the experimental geometries. The geometries are taken from the IP131 database.[18] The nine molecules (C_4H_5N, C_6H_6, CF_3CN, $CH_2ClCH_2CH_3$, $CH_3CH(CH_3)CH_3$, CH_3CONH_2, CH_3SOCH_3, $N(CH_3)_3$, SF_6) were excluded because of the excessive computational resources needed. The coupled-cluster theory with iterative singles and doubles (CCSD)[19–21] and equation-of-motion CCSD (EOM-CCSD),[22–30] are employed as the benchmarks for the electronic and optical properties, respectively.

We examine the vertical ionization potentials (IP), vertical electron affinities (EA), fundamental gaps (E_g), optical gaps (E_{opt}), and exciton binding energies (E_b) of 121 molecules using various density functional methods. The IP, EA, and E_g calculations follows the procedure detailed in our previous work.[31] For the KS-DFT and TDDFT calculations, we adopt popular density functionals, involving the local-density-approximation (LDA[32,33]) functional, a generalized-gradient-approximation (GGA) functional (PBE[34,35]), a meta-GGA functional (M06-L[36]), a global hybrid GGA functional (B3LYP[16,17]), three long-range corrected (LC) hybrid GGA functionals (ωB97,[37] ωB97X,[37] and ωB97X-D[38]), and two global hybrid meta-GGA functionals (M06-HF[36,39] and M06-2X[40]).

All calculations are performed using the Gaussian09 program.[41] Results are computed using the aug-cc-pVQZ basis set with the ultrafine grid, EML (99 590), consisting of 99 Euler–Maclaurin radial grid points[42] and 590 Lebedev angular grid points.[43–45] All the calculated results are provided in the ESI (Tables S1–S12†). The error for each entry is defined as error = theoretical value − reference value. The notations used for characterizing statistical errors are as follows: mean signed errors (MSEs), mean absolute errors (MAEs), and root-mean-square (RMS) errors.

A. Vertical ionization potentials

The vertical ionization potential (IP) of a neutral molecule is defined as the energy difference between the cationic and neutral charge states,

$$\mathrm{IP}(1) = E_{\mathrm{tot}}\,(\mathrm{cation}) - E_{\mathrm{tot}}\,(\mathrm{neutral}). \quad (1)$$

For the exact KS-DFT, the vertical IP of a neutral molecule is the same as the minus HOMO (highest occupied molecular orbital) energy of the neutral molecule,[32,46]

$$\mathrm{IP}(2) = -E_{\mathrm{HOMO}}\,(\mathrm{neutral}) \quad (2)$$

Therefore, IP(2) is the same as IP(1) for the exact KS-DFT. For approximate density functional methods, IP(1) and IP(2) may be adopted to examine the accuracy of the predicted total energies and HOMO energies, respectively.

B. Vertical electron affinities

The vertical electron affinity (EA) of a neutral molecule is defined as the energy difference between the neutral and anionic charge states,

$$\mathrm{EA}(1) = E_{\mathrm{tot}}\,(\mathrm{neutral}) - E_{\mathrm{tot}}\,(\mathrm{anion}). \quad (3)$$

By comparing eqn (1) with (3), the vertical EA of a neutral molecule is identical to the vertical IP of the anion, which is, for the exact KS-DFT, the minus HOMO energy of the anion,

$$\mathrm{EA}(2) = -E_{\mathrm{HOMO}}\,(\mathrm{anion}). \quad (4)$$

For the exact KS-DFT, EA(2) is identical to EA(1). Therefore, EA(1) and EA(2) may be adopted to examine the accuracy of approximate density functional methods on total energies and HOMO energies, respectively.

In addition, the vertical EA of a neutral molecule is conventionally approximated by the minus LUMO (lowest unoccupied molecular orbital) energy of the neutral molecule,[18]

$$\mathrm{EA}(3) = -E_{\mathrm{LUMO}}\,(\mathrm{neutral}). \quad (5)$$

However, even for the exact KS-DFT, a difference exists between EA(3) and vertical EA due to the derivative discontinuity (DD) of the exchange–correlation functional.[47–50] Recent study shows that DD is close to zero for LC hybrid functionals,[51] so the EA(3) calculated by a LC hybrid functional should be close to the true vertical EA.

C. Fundamental gaps

The fundamental gap (E_g) of a molecule is defined as the difference between the vertical IP and vertical EA of the molecule,

$$E_g = \mathrm{IP} - \mathrm{EA}. \quad (6)$$

Since there are many different ways of calculating vertical IP and vertical EA from density functional methods, we have mainly three ways of calculating E_g:

$$E_g(1) = \mathrm{IP}(1) - \mathrm{EA}(1) = E_{\mathrm{tot}}\,(\mathrm{cation}) + E_{\mathrm{tot}}\,(\mathrm{anion}) - 2E_{\mathrm{tot}}\,(\mathrm{neutral}) \quad (7)$$

$$E_g(2) = \mathrm{IP}(2) - \mathrm{EA}(2) = E_{\mathrm{HOMO}}\,(\mathrm{anion}) - E_{\mathrm{HOMO}}\,(\mathrm{neutral}) \quad (8)$$

$$E_g(3) = \mathrm{IP}(2) - \mathrm{EA}(3) = E_{\mathrm{LUMO}}\,(\mathrm{neutral}) - E_{\mathrm{HOMO}}\,(\mathrm{neutral}) \quad (9)$$

Note that $E_g(3)$ is the so-called Kohn–Sham (KS) gap or HOMO–LUMO gap in KS-DFT.[18,52]

As mentioned previously, for LC hybrid functionals, EA(3) should be close to vertical EA, and hence $E_g(3)$ should be close to the true E_g.

D. Optical gaps

The optical gap (E_{opt}) of a molecule, defined by a neutral excitation, is the energy difference between the lowest dipole-allowed excited state and the ground state,

$$E_{opt} = E_{tot}\,(\text{neutral, excited}) - E_{tot}\,(\text{neutral}). \quad (10)$$

As E_{opt} is an excited-state property, it cannot be directly calculated using CCSD or KS-DFT. To be consistent with the ground-state calculations, we adopt EOM-CCSD[22–30] and TDDFT[53–60] (with the same density functionals for the ground-state calculations) to calculate the E_{opt}.

E. Exciton binding energies

The exciton binding energy (E_b) of a molecule is defined as the difference between the fundamental and optical gaps,

$$E_b = E_g - E_{opt}. \quad (11)$$

As there are three ways of calculating E_g (see eqn (7)–(9)), E_b can also be calculated in three ways, *i.e.*,

$$E_b(1) = E_g(1) - E_{opt} \quad (12)$$

$$E_b(2) = E_g(2) - E_{opt} \quad (13)$$

$$E_b(3) = E_g(3) - E_{opt} \quad (14)$$

It is important to note that $E_b(1)$, $E_b(2)$, and $E_b(3)$ obtained with density functional methods are closely related to the calculated $E_g(1)$, $E_g(2)$, and $E_g(3)$, respectively. For the exact KS-DFT, as IP(2) is identical to IP(1), and EA(2) is identical to EA(1), $E_g(2)$ is the same as $E_g(1)$, the exact E_g. Therefore, for the exact KS-DFT and TDDFT, $E_b(2)$ should be identical to $E_b(1)$, the exact E_b. Consequently, the errors in the calculated $E_g(1)$, $E_g(2)$, $E_b(1)$, and $E_b(2)$ are directly related to the accuracy of the exchange–correlation functional adopted in KS-DFT and TDDFT. However, due to the lack of the DD in the calculated KS gap, $E_g(3)$ tends to be smaller than $E_g(1)$ (the true fundamental gap), even for the exact KS-DFT. Accordingly, when the calculated KS gap ($E_g(3)$) is less than E_{opt}, one obtains an unphysical negative value of E_b. We show that this is indeed frequently observed for local and semilocal density functional methods. However, as the DD is close to zero for LC hybrid functionals (which belong to the generalized Kohn–Sham (GKS) method, not the "pure" KS-DFT), $E_g(3)$ and $E_b(3)$ calculated using LC hybrid functionals are expected to be close to the true E_g and E_b, respectively.

III. Results and discussion

A. Benchmark methods

The IP(1) calculated from CCSD and CCSD(T) are compared to experimental values for the 121 molecules (see Fig. S1 and Table S13 in ESI†). Both methods are very accurate with MAE being 0.17 eV from CCSD and 0.14 eV from CCSD(T). The difference between these two methods are around 0.1 eV for IP(1) and $E_g(1)$, and around 0.05 eV for EA(1) (see Fig. S1 and Table S14 ESI†). Such differences are much smaller than those associated with density functional methods (usually greater than 0.5 eV). Therefore, we believe that the CCSD results can be taken as benchmarks. In this study, CCSD and EOM-CCSD (*i.e.*, for consistency with CCSD) are adopted as the benchmarking methods for the ground-state and excited-state properties, respectively.

B. Accuracy of density functional methods

Five optoelectronic properties, including the vertical ionization potentials, vertical electron affinities, fundamental gaps, optical gaps, and exciton binding energies of 121 molecules are adopted to examine the accuracy of various density functionals in KS-DFT and TDDFT.

The accuracy of various density functionals with respect to experimental values on IP(1) and IP(2) are summarized in Table S15 in ESI.† Despite the fact that different measures of accuracy yield slightly different ranks in performance of IP(1), M06-2X and ωB97X-D are among the most accurate density functionals, with an MAE of around 0.18 eV. LDA is the least accurate with an MAE of 0.56 eV, which is more than three times the error of the best functional. It is also interesting to note that while M06-HF and M06-2X are both hybrid meta-GGA functionals, the MAE of M06-HF (0.46 eV) is more than twice that of M06-2X (0.18 eV).

There is a significant variation in the performance when the ionization potentials are estimated from the HOMO energy (IP(2)). The ωB97 functional is the best functional with an MAE of 0.42 eV. PBE is the least accurate with an MAE of 4.44 eV, which is more ten times higher than that of the best functional here. The MAE difference in IP(1) between M06-HF and M06-2X is more than twice, but the performance of M06-HF (0.99 eV) and M06-2X (1.51 eV) is similar for IP(2). In general, the MAE in IP(2) is 2 to 13 times larger than those for IP(1).

Since there are no comprehensive experimental data available for the other properties, the results from CCSD are taken as the reference values for evaluating the performance of density functional methods. Table 1 shows such comparison for the vertical ionization potentials, vertical electron affinities, fundamental gaps, optical gaps, and exciton binding energies. Fig. 1–5 illustrates the MAE in IP, EA, E_g, E_{opt}, and E_b with different definitions. For IP(1), M06-2X agrees best with CCSD with an MAE difference of 0.13 eV. The ωB97 series also provide quite consistent results with CCSD with MAE difference being about 0.16 eV. For EA(1), the performance of M06-2X and the ωB97 series are among the best, with the ωB97X-D being the best functional (MAE = 0.16 eV). The ωB97X and M06-2X show the best performance for $E_g(1)$ are shown that ωB97X (MAE = 0.26 eV) and M06-2X (MAE = 0.27 eV) are the best functionals. The LDA yields the worst results for IP(1) and EA(1); however, the PBE is the least accurate for $E_g(1)$ because it generally underestimates IP(1) (MAE = 0.42 eV, MSE = −0.31 eV) but overestimates EA(1) (MAE = 0.34 eV, MSE = 0.32 eV). In summary, M06-2X and the ωB97 series (ωB97, ωB97X, and ωB97X-D) are the best density functionals for the ground-state properties (with an accuracy of 0.3 eV or less). Furthermore,

Table 1 Statistical errors (in eV) of 9 density functional methods for various properties (with respect to the CCSD or EOM-CCSD data)

	Error	LDA	PBE	M06L	B3LYP	ωB97	ωB97X	ωB97X-D	M06-2X	M06-HF
IP(1)	MSE	0.39	−0.31	−0.36	−0.09	−0.07	−0.07	−0.09	**0.03**	0.35
	MAE	0.58	0.42	0.39	0.26	0.16	0.17	0.20	**0.13**	0.37
	RMS	0.66	0.61	0.56	0.37	0.23	0.24	0.28	**0.18**	0.46
IP(2)	MSE	−3.92	−4.50	−4.35	−3.25	**−0.34**	−0.59	−1.12	−1.57	0.84
	MAE	3.92	4.50	4.35	3.25	**0.41**	0.59	1.13	1.57	0.91
	RMS	4.05	4.61	4.45	3.32	**0.67**	0.82	1.28	1.63	1.04
EA(1)	MSE	0.78	0.32	−0.07	0.30	**0.02**	0.07	0.13	0.05	0.17
	MAE	0.79	0.34	0.24	0.31	0.20	0.18	**0.16**	0.21	0.33
	RMS	0.86	0.46	0.38	0.43	0.34	0.32	**0.31**	0.37	0.42
EA(2)	MSE	−1.27	−1.62	−1.92	−1.22	0.13	0.12	**0.00**	−0.75	0.34
	MAE	1.31	1.67	1.95	1.28	0.24	**0.20**	0.24	0.80	0.55
	RMS	1.60	1.97	2.20	1.47	0.39	**0.35**	0.39	0.87	0.76
EA(3)	MSE	3.15	2.53	2.87	1.95	−0.07	**−0.03**	0.24	1.25	1.75
	MAE	3.15	2.53	2.87	1.96	**0.29**	0.34	0.42	1.26	1.80
	RMS	3.44	2.81	8.90	2.15	**0.37**	0.41	0.56	1.80	5.57
$E_g(1)$	MSE	−0.39	−0.63	−0.29	−0.39	−0.09	−0.14	−0.22	**−0.02**	0.18
	MAE	0.51	0.65	0.44	0.45	0.28	**0.26**	0.30	0.27	0.33
	RMS	0.71	0.88	0.62	0.62	0.42	0.41	0.44	**0.40**	0.46
$E_g(2)$	MSE	−5.46	−2.88	−2.43	−2.03	**−0.47**	−0.71	−1.13	−0.82	0.49
	MAE	6.14	2.88	2.43	2.03	**0.58**	0.73	1.13	0.86	0.75
	RMS	8.08	3.14	2.70	2.22	**0.82**	0.94	1.30	1.01	0.95
$E_g(3)$	MSE	−7.07	−7.03	−7.22	−5.19	**−0.27**	−0.56	−1.36	−2.82	−0.92
	MAE	7.07	7.03	7.22	5.19	**0.51**	0.64	1.39	2.82	1.57
	RMS	7.32	7.25	11.25	5.35	**0.77**	0.93	1.61	3.21	5.66
E_{opt}	MSE	−0.91	−1.05	−0.61	−0.63	**−0.13**	−0.15	−0.33	−0.38	−0.44
	MAE	0.97	1.12	0.70	0.76	**0.31**	0.32	0.46	0.46	0.68
	RMS	1.15	1.29	0.90	0.92	0.55	0.63	0.71	**0.54**	1.05
$E_b(1)$	MSE	0.52	0.42	0.32	0.24	0.04	**0.01**	0.12	0.36	0.62
	MAE	0.66	0.66	0.57	0.53	0.39	**0.38**	0.40	0.48	0.80
	RMS	0.88	0.88	0.74	0.78	0.71	0.71	0.71	**0.61**	1.16
$E_b(2)$	MSE	−1.74	−1.83	−1.82	−1.39	**−0.34**	−0.56	−0.79	−0.43	0.93
	MAE	1.77	1.85	1.86	1.42	**0.53**	0.66	0.87	0.57	1.17
	RMS	2.05	2.13	2.12	1.66	0.81	0.92	1.11	**0.71**	1.49
$E_b(3)$	MSE	−6.16	−5.98	−6.62	−4.56	**−0.13**	−0.41	−1.03	−2.44	−0.48
	MAE	6.16	5.98	6.62	4.56	**0.48**	0.59	1.11	2.44	1.69
	RMS	6.48	6.28	10.91	4.80	**0.74**	0.96	1.46	2.86	5.69
Total	MSE	−1.84	−1.88	−1.87	−1.36	**−0.14**	−0.25	−0.47	−0.63	0.32
	MAE	2.75	2.47	2.47	1.83	**0.36**	0.42	0.65	0.99	0.91
	RMS	4.08	3.45	5.50	2.57	**0.60**	0.69	0.96	1.52	2.93

as in the case of IP, the MAE from the least accurate methods (often LDA and GGAs) can be more than twice that of the best functional.

The optical gap is a measure of performance in describing the excited state. The ωB97 and ωB97X functionals perform the best for optical gaps. PBE shows surprisingly poor results for

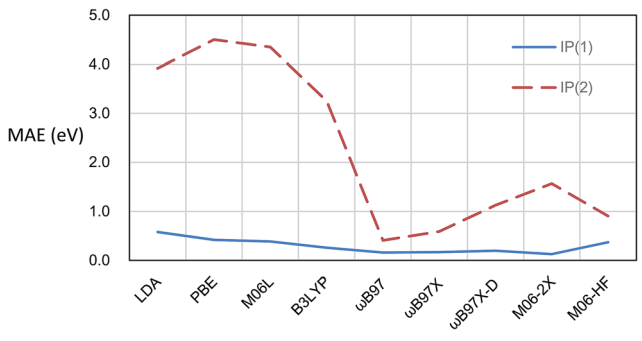

Fig. 1 Comparison of MAE in ionization potential (IP) from 9 DFT methods with respective to CCSD. IP(1) (blue solid line) is calculated from eqn (1) and IP(2) (red dashed line) from eqn (2).

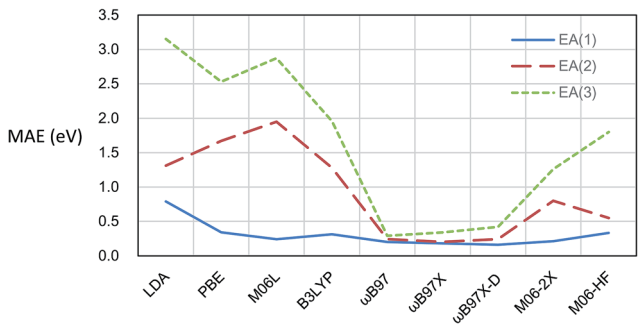

Fig. 2 Comparison of MAE in electron affinity (EA) from 9 DFT methods with respective to CCSD. EA(1) (blue solid line) is calculated from eqn (3), EA(2) (red dashed line) from eqn (4), and EA(3) from eqn (5).

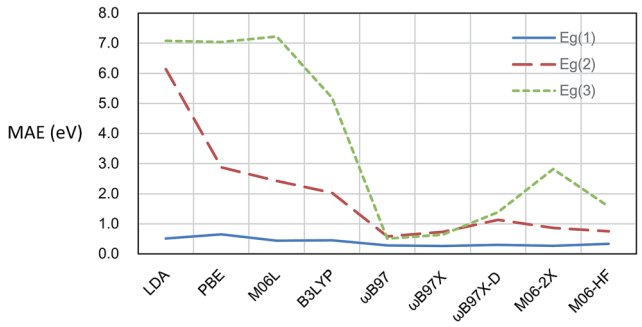

Fig. 3 Comparison of MAE in fundamental gap (E_g) from 9 DFT methods with respective to CCSD. $E_g(1)$ (blue solid line) is calculated from eqn (7), $E_g(2)$ (red dashed line) from eqn (8), and $E_g(3)$ from eqn (9).

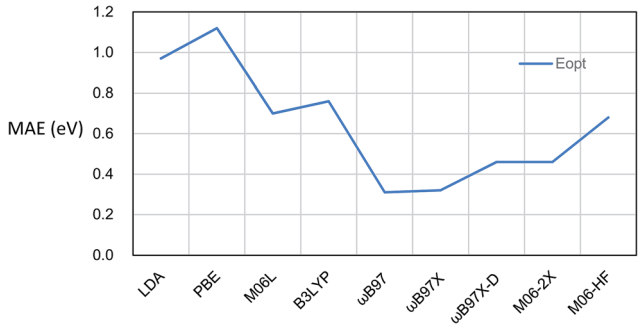

Fig. 4 Comparison of MAE in optical gap (E_{opt} from eqn (10)) from 9 DFT methods with respective to EOM-CCSD.

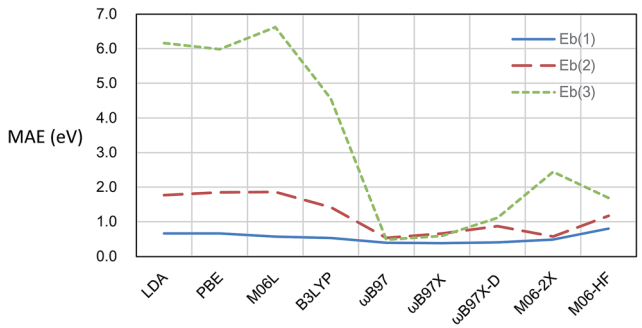

Fig. 5 Comparison of MAE in binding energy (E_b) from 9 DFT methods with respective to CCSD and EOM-CCSD. $E_b(1)$ (blue solid line) is calculated from eqn (12), $E_b(2)$ (red dashed line) from eqn (13), and $E_b(3)$ from eqn (14).

E_{opt}, with an MAE (1.12 eV) that is three times higher than the best method. It is useful to note that the electron–hole attraction which stabilizes the exciton is not explicitly present in the TDDFT kernel associated with the standard local or semilocal density functional (*e.g.*, LDA or PBE). There are efforts made to include electron–hole attraction and binding energies based on the Bethe–Salpeter formalism[61,62] or on developing new TDDFT kernels.[63–65]

Since ωB97 and ωB97X perform the best for both $E_g(1)$ and E_{opt}, unsurprisingly, they are the most accurate methods for $E_b(1)$. ωB97X-D has 0.1 eV more than ωB97 and ωB97X for E_{opt}, but ωB97X-D also has good performance as ωB97 and ωB97X. The MAE in $E_b(1)$ from M06-HF (0.80 eV) is more than twice larger than that from ωB97X. It is interesting to note that while B3LYP is inaccurate for $E_g(1)$ (MAE = 0.45 eV) and E_{opt} (MAE = 0.76 eV), it is reasonably accurate for $E_b(1)$ (MAE = 0.53 eV), which is a result of systematic underestimation IP(1) (MAE = 0.26 eV, MSE = 0.09 eV), EA(1) (MAE = 0.31 eV, MSE = 0.30 eV), $E_g(1)$ (MAE = 0.45 eV, MSE = −0.39 eV), and E_{opt} (MAE = 0.76 eV, MSE = −0.63 eV). In summary, the ωB97 functional provides the most reliable predictions for total energy of a molecule both in the ground state and in the excited state.

The performance in IP(2), EA(2), $E_g(2)$, and $E_b(2)$ is an indication of the quality of HOMO energy. In general, the MAE for IP(2) is 3 to 9 times larger than those for IP(1). ωB97 is the best functional for IP(2) with an MAE of 0.41 eV (compared to 0.16 for IP(1)). The ωB97X-D underestimated the HOMO energy, resulting in a large error in IP(2) (MAE = 1.13 eV and MSE = −1.12 eV), $E_g(2)$ and $E_b(2)$. The MAE errors from ωB97 methods for EA(2) are quite similar to those for EA(1). However, LDA, PBE, M06L, and B3LYP show significantly increased inaccuracy in EA(2). As a result, these methods are also poor for $E_g(2)$ and $E_b(2)$. The ωB97 is the best functional for $E_g(2)$ (MAE = 0.58 eV) and $E_b(2)$ (MAE = 0.53 eV). The global hybrid MGGA functionals, M06-2X and M06-HF, also provide reasonable accuracy in the HOMO energies. However, since M06-2X underestimates for E_{opt} and E_g, it is accurate for $E_b(2)$ which is also a result of systematic underestimation.

The performance in EA(3), $E_g(3)$, and $E_b(3)$ implies the description accuracy in the LUMO energy. The performance of ωB97 series in these properties are quite similar to the corresponding EA(2), $E_g(2)$, and $E_b(2)$. However, all other methods, including hybrid MGGA methods, show significantly increased MAEs here. For example, the MAE of EA(3) from M06-HF (1.80 eV) is almost 3 times higher than that of EA(2) (0.55 eV). Therefore, the ωB97 series provide reliable description for the LUMO energy.

It is noteworthy that in some cases the calculated LUMO energies are so small that $E_g(3)$ becomes smaller than optical gap, yielding qualitatively incorrect exciton binding energies (*i.e.*, E_b can be negative!). 115 out of 121 from LDA, 116 out of 121 from PBE, 112 out of 121 from M06L, 38 out of 121 from B3LYP, 10 out of 121 from M06-2X and 7 out of 121 from M06-HF, 2 out of 121 from ωB97 and ωB97X, 5 out of 121 from ωB97X-D show negative $E_b(3)$ (see Table S12† for a complete list of all the $E_b(3)$). In some cases, the calculated LUMO energies are even lower than the calculated HOMO energies from M06 methods (M06L, M06-HF, M06-2X), resulting in incorrect negative $E_g(3)$ (−87.12 eV (hydrogen atom) from M06L, −5.00 eV (hydrogen atom) from M06-2X and −40.36 eV (hydrogen atom), −18.76 eV (lithium atom), −13.04 eV (sodium atom) from M06-HF).

It is worthwhile to note that LC hybrid functionals with non-empirical optimization of the range-separation parameter ω have been recently developed,[66,67] and have yielded accurate

exciton binding energies and quasiparticle energies with respect to experiment.[68,69] While the performance of these LC hybrid functionals have not been examined in this work, we expect that these LC hybrid functionals should also yield accurate results for the properties studied.

IV. Conclusions

In conclusion, we have examined the performance of several density functional methods on the exciton binding energies and related optoelectronic properties of 121 small- to medium-sized molecules. Relative to the highly accurate CCSD and EOM-CCSD methods, ωB97, ωB97X, and ωB97X-D exhibit the best accuracy for these properties. However, when intermolecular charge-transfer excitons are involved, ωB97X-D, which includes dispersion corrections, is expected to be essential.

Acknowledgements

We thank the support from the Ministry of Science and Technology of Taiwan (Grant No. MOST104-2221-E-002-186-MY3 and MOST104-2628-M-002-011-MY3), National Taiwan University (Grant No. NTU-CDP-104R7876 and NTU-CDP-104R7818), and the National Center for Theoretical Sciences of Taiwan. The computational resources from the National Center for High-Performance Computing of Taiwan and the Computing and Information Networking Center of the National Taiwan University are acknowledged.

References

1 M. Knupfer, *Appl. Phys. A: Mater. Sci. Process.*, 2003, **77**, 623–626.
2 A. Franceschetti and A. Zunger, *Phys. Rev. Lett.*, 1997, **78**, 915–918.
3 B. A. Gregg, *J. Phys. Chem. B*, 2003, **107**, 4688–4698.
4 I. G. Hill, A. Kahn, Z. G. Soos and R. A. Pascal, *Chem. Phys. Lett.*, 2000, **327**, 181–188.
5 B. Schweitzer and H. Bassler, *Synth. Met.*, 2000, **109**, 1–6.
6 G. Weiser, *Phys. Rev. B: Condens. Matter Mater. Phys.*, 1992, **45**, 14076–14085.
7 S. F. Alvarado, P. F. Seidler, D. G. Lidzey and D. D. C. Bradley, *Phys. Rev. Lett.*, 1998, **81**, 1082–1085.
8 M. Liess, S. Jeglinski, Z. V. Vardeny, M. Ozaki, K. Yoshino, Y. Ding and T. Barton, *Phys. Rev. B: Condens. Matter Mater. Phys.*, 1997, **56**, 15712–15724.
9 P. I. Djurovich, E. I. Mayo, S. R. Forrest and M. E. Thompson, *Org. Electron.*, 2009, **10**, 515–520.
10 P. K. Nayak, *Synth. Met.*, 2013, **174**, 42–45.
11 P. K. Nayak and N. Periasamy, *Org. Electron.*, 2009, **10**, 1396–1400.
12 P. Hohenberg and W. Kohn, *Phys. Rev. B: Condens. Matter Mater. Phys.*, 1964, **136**, B864–B871.
13 W. Kohn and L. J. Sham, *Phys. Rev.*, 1965, **140**, A1133–A1138.
14 M. E. Casida, *Recent Advances in Density Functional Methods, Part I*, World Scientific, Singapore, 1995.
15 E. K. U. Gross, J. F. Dobson and M. Petersilka, *Density Functional Theory Ii*, 1996, **181**, 81–172.
16 A. D. Becke, *J. Chem. Phys.*, 1993, **98**, 5648–5652.
17 P. J. Stephens, F. J. Devlin, C. F. Chabalowski and M. J. Frisch, *J. Phys. Chem.*, 1994, **98**, 11623–11627.
18 Y.-S. Lin, C.-W. Tsai, G.-D. Li and J.-D. Chai, *J. Chem. Phys.*, 2012, **136**, 154109.
19 G. D. Purvis and R. J. Bartlett, *J. Chem. Phys.*, 1982, **76**, 1910–1918.
20 G. E. Scuseria, C. L. Janssen and H. F. Schaefer, *J. Chem. Phys.*, 1988, **89**, 7382–7387.
21 G. E. Scuseria and H. F. Schaefer, *J. Chem. Phys.*, 1989, **90**, 3700–3703.
22 H. Koch and P. Jorgensen, *J. Chem. Phys.*, 1990, **93**, 3333–3344.
23 J. F. Stanton and R. J. Bartlett, *J. Chem. Phys.*, 1993, **98**, 7029–7039.
24 H. Koch, R. Kobayashi, A. S. Demeras and P. Jorgensen, *J. Chem. Phys.*, 1994, **100**, 4393–4400.
25 M. Kallay and J. Gauss, *J. Chem. Phys.*, 2004, **121**, 9257–9269.
26 M. Caricato, *J. Chem. Theory Comput.*, 2012, **8**, 5081–5091.
27 M. Caricato, *J. Chem. Theory Comput.*, 2012, **8**, 4494–4502.
28 M. Caricato, F. Lipparini, G. Scalmani, C. Cappelli and V. Barone, *J. Chem. Theory Comput.*, 2013, **9**, 3035–3042.
29 M. Caricato, *J. Chem. Phys.*, 2013, **139**, 044116.
30 M. Caricato, *J. Chem. Phys.*, 2013, **139**, 114103.
31 C.-W. Tsai, Y.-C. Su, G.-D. Li and J.-D. Chai, *Phys. Chem. Chem. Phys.*, 2013, **15**, 8352–8361.
32 R. G. Parr and W. Yang, *Density Functional Theory of Atoms and Molecules*, Oxford University Press, New York, 1989.
33 R. M. Dreizler and E. K. U. Gross, *Density Functional Theory*, Springer-Verlag, 1990.
34 J. P. Perdew, K. Burke and M. Ernzerhof, *Phys. Rev. Lett.*, 1996, **77**, 3865–3868.
35 J. P. Perdew, K. Burke and M. Ernzerhof, *Phys. Rev. Lett.*, 1997, **78**, 1396.
36 Y. Zhao and D. G. Truhlar, *J. Phys. Chem. A*, 2006, **110**, 13126–13130.
37 J.-D. Chai and M. Head-Gordon, *J. Chem. Phys.*, 2008, **128**, 084106.
38 J.-D. Chai and M. Head-Gordon, *Phys. Chem. Chem. Phys.*, 2008, **10**, 6615–6620.
39 Y. Zhao and D. G. Truhlar, *J. Phys. Chem. A*, 2006, **110**, 5121–5129.
40 Y. Zhao and D. G. Truhlar, *Theor. Chem. Acc.*, 2008, **120**, 215–241.
41 G. W. T. M. J. Frisch, H. B. Schlegel, G. E. Scuseria, J. R. C. M. A. Robb, G. Scalmani, V. Barone, B. Mennucci, H. N. G. A. Petersson, M. Caricato, X. Li, H. P. Hratchian, J. B. A. F. Izmaylov, G. Zheng, J. L. Sonnenberg, M. Hada, K. T. M. Ehara, R. Fukuda, J. Hasegawa, M. Ishida, T. Nakajima, O. K. Y. Honda, H. Nakai, T. Vreven, J. A. Montgomery Jr, F. O. J. E. Peralta, M. Bearpark, J. J. Heyd, E. Brothers, V. N. S. K. N. Kudin, R. Kobayashi, J. Normand, A. R. K. Raghavachari, J. C. Burant, S. S. Iyengar, J. Tomasi, N. R. M. Cossi, J. M. Millam,

M. Klene, J. E. Knox, J. B. Cross, C. A. V. Bakken, J. Jaramillo, R. Gomperts, R. E. Stratmann, A. J. A. O. Yazyev, R. Cammi, C. Pomelli, J. W. Ochterski, K. M. R. L. Martin, V. G. Zakrzewski, G. A. Voth, J. J. D. P. Salvador, S. Dapprich, A. D. Daniels, J. B. F. O. Farkas, J. V. Ortiz, J. Cioslowski and a. D. J. Fox, *Gaussian 09, Revision A.02*, Gaussian, Inc., Wallingford CT, 2009.

42 C. W. Murray, N. C. Handy and G. J. Laming, *Mol. Phys.*, 1993, **78**, 997–1014.

43 V. I. Lebedev, *Sibirsk. Mat. Zh.*, 1977, **16**, 293.

44 V. I. Lebedev and Z. Vychisl, *Mat. Mat. Fiz.*, 1976, **16**, 293.

45 V. I. Lebedev and Z. Vychisl, *Mat. Mat. Fiz.*, 1975, **15**, 48.

46 M. Levy, J. P. Perdew and V. Sahni, *Phys. Rev. A*, 1984, **30**, 2745–2748.

47 L. J. Sham and M. Schluter, *Phys. Rev. Lett.*, 1983, **51**, 1888–1891.

48 L. J. Sham and M. Schluter, *Phys. Rev. B: Condens. Matter Mater. Phys.*, 1985, **32**, 3883–3889.

49 J. P. Perdew and M. Levy, *Phys. Rev. Lett.*, 1983, **51**, 1884–1887.

50 J.-D. Chai and P.-T. Chen, *Phys. Rev. Lett.*, 2013, **110**, 033002.

51 T. Tsuneda, J.-W. Song, S. Suzuki and K. Hirao, *J. Chem. Phys.*, 2010, **133**, 174101.

52 J. P. Perdew and M. Levy, *Phys. Rev. Lett.*, 1983, **51**, 1884–1887.

53 E. Runge and E. K. U. Gross, *Phys. Rev. Lett.*, 1984, **52**, 997–1000.

54 G. Scalmani, M. J. Frisch, B. Mennucci, J. Tomasi, R. Cammi and V. Barone, *J. Chem. Phys.*, 2006, **124**, 094107.

55 F. Furche and R. Ahlrichs, *J. Chem. Phys.*, 2002, **117**, 7433–7447.

56 C. Van Caillie and R. D. Amos, *Chem. Phys. Lett.*, 2000, **317**, 159–164.

57 C. Van Caillie and R. D. Amos, *Chem. Phys. Lett.*, 1999, **308**, 249–255.

58 R. E. Stratmann, G. E. Scuseria and M. J. Frisch, *J. Chem. Phys.*, 1998, **109**, 8218–8224.

59 M. E. Casida, C. Jamorski, K. C. Casida and D. R. Salahub, *J. Chem. Phys.*, 1998, **108**, 4439–4449.

60 R. Bauernschmitt and R. Ahlrichs, *Chem. Phys. Lett.*, 1996, **256**, 454–464.

61 D. Jacquemin, I. Duchemin and X. Blase, *J. Chem. Theory Comput.*, 2015, **11**, 3290–3304.

62 G. Onida, L. Reining and A. Rubio, *Rev. Mod. Phys.*, 2002, **74**, 601–659.

63 A. Marini, R. Del Sole and A. Rubio, *Phys. Rev. Lett.*, 2003, **91**, 4.

64 F. Sottile, V. Olevano and L. Reining, *Phys. Rev. Lett.*, 2003, **91**, 4.

65 D. Varsano, A. Marini and A. Rubio, *Phys. Rev. Lett.*, 2008, **101**, 4.

66 T. Stein, L. Kronik and R. Baer, *J. Chem. Phys.*, 2009, **131**, 5.

67 T. Stein, L. Kronik and R. Baer, *J. Am. Chem. Soc.*, 2009, **131**, 2818–2820.

68 B. M. Wong and T. H. Hsieh, *J. Chem. Theory Comput.*, 2010, **6**, 3704–3712.

69 N. Kuritz, T. Stein, R. Baer and L. Kronik, *J. Chem. Theory Comput.*, 2011, **7**, 2408–2415.